Talanta 214 (2020) 120810

Contents lists available at ScienceDirect

Talanta

journal homepage: www.elsevier.com/locate/talanta

Flex-GO (Flexible graphene oxide) sensor for electrochemical monitoring lactate in low-volume passive perspired human sweat

Kai-Chun Lin[a], Sriram Muthukumar[b], Shalini Prasad[a,*]

[a] Department of Bioengineering, University of Texas at Dallas, 800 West Campbell Road, Richardson, TX, 75080, USA
[b] Enlisense LLC, 1813 Audubon Pond Way, Allen, TX, 75013, USA

ARTICLE INFO

Keywords:
Graphene oxide
Lactate
Electrochemical impedance spectroscopy
Perspired human sweat
Biosensor

ABSTRACT

In this work, a low volume, sweat lactate sensor functioning on passively expressed eccrine sweat was designed, fabricated and tested in human sweat and its performance was benchmarked against a standard reference; Lactate Plus meter. This novel sensor comprises of graphene oxide (GO) nanosheets integrated into a nanoporous flexible electrode system for low-volume (1–5 μL) ultrasensitive impedance based detection of lactate using non-faradaic electron-ionic charge transfer. Lactate oxidase (LOD) enzyme was immobilized on the surface of GO nanosheets towards developing an affinity biosensor specific to the physiological relevant range (4–80 mM) of lactate in perspired human sweat. Sensing was achieved by measuring impedance changes specific to lactate binding along the GO nanosheet interface using electrochemical impedance spectroscopy. The sensor demonstrated a dynamic range from 1 to 100 mM spiked in synthetic and human sweat with a limit of detection of 1 mM. A specificity study conducted using cortisol expressed in sweat revealed a negative response to the lactate oxidase. Continuous lactate sensing studies were performed during which the sensor was responsive to concentrations of lactate up to 138.6 mM. Correlation of the sensor response with actual lactate concentration (1.3–113.4 mM) was found to be 0.955.

1. Introduction

Lactate is a product of the anaerobic glycolysis resulting from pyruvate to lactate by the enzyme lactate dehydrogenase (LDH) and can be found in blood and other biological fluids. Lactate metabolism provides clues towards determining multiple physiological processes resulting in varied disease states within the human body. Some of these are muscle fatigue, sepsis, wound repair, regeneration, etc [1]. Lactate is the most important gluconeogenic precursor (new glucose generator) in the body, hence it is especially relevant and a highly attractive biomarker that merits temporal monitoring leading to a dynamic assessment of lactate level variation [2]. Lactate is controlled for patients with lactic acidosis [3,4], and for calculating lactate anaerobic thresholds [5,6]. The physiological concentration of lactate in blood ranges from 0.6 to 2.0 mM but can rise quickly up to 20–30 mM during physical activity [7]. Lactate concentration can be measured off line in blood, plasma, sweat or urine using laboratory device such as gas chromatography (GC), and high-performance liquid chromatography (HPLC) [8,9]. However, the size of these instruments is quite large and the analytical methods for the sample treatment are tedious.

Commercially available biosensors for blood lactate have been developed and provide quick results, but require an invasive or minimally invasive method of sample collection. This issue for real-time monitoring methods has guided researchers to test other body fluids [10]. Human sweat contains abundant information about a person's health status and thus is an excellent biofluid for non-invasive chemosensing [11]. Continuous detection of sodium, lactate, ammonium, and calcium is highly desired for optimal physiological balance [12–15]. Sweat has also been used for monitoring a person's intoxication level [16] and signs of drug abuse [17], among other applications. Wearable, non-invasive sensors are therefore needed for such sweat monitoring [14].

Sweat lactate is a function of eccrine gland energy metabolism; an increase in the exercise intensity leads to increased production of sweat lactate [18]. Perspiration may thus be suitably utilized for the analysis of physical performance in individuals without the need for an invasive blood sampling approach [19]. Sweat lactate can also serve as a sensitive marker of tissue viability and may provide warning for pressure ischemia, reflecting the insufficient oxidative metabolism and a compromise of tissue viability [20–22]. However, there are new challenges raised in detecting lactate in sweat, such as low-volume and higher physiological relevant range (4–80 mM) of lactate in perspired human

* Corresponding author.
E-mail address: Shalini.Prasad@utdallas.edu (S. Prasad).

https://doi.org/10.1016/j.talanta.2020.120810
Received 23 December 2019; Received in revised form 30 January 2020; Accepted 5 February 2020
Available online 08 February 2020
0039-9140/

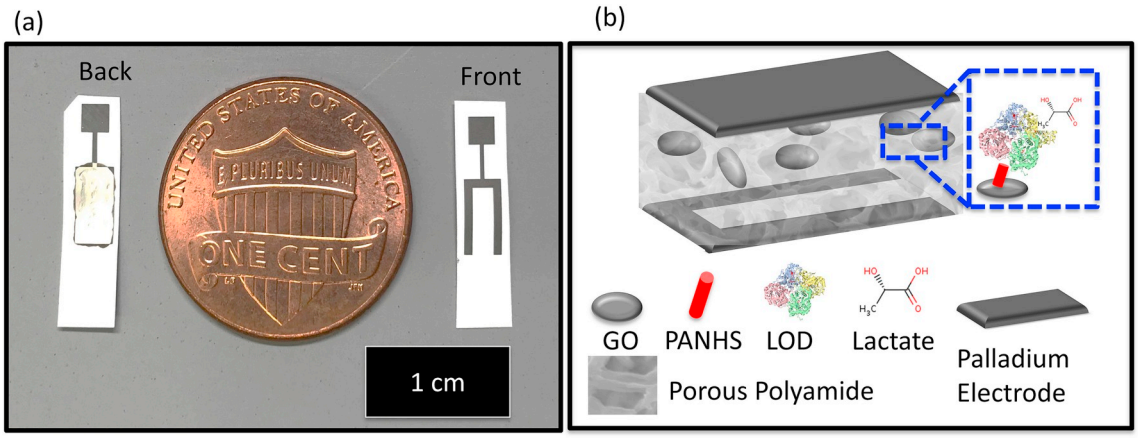

Fig. 1. (a) Optical visualization of the lactate sweat sensor. **(b)** Schematic drawing of the Graphene oxide-through membrane sensing platform for electrochemical affinity-based detection of lactate. The picture depicts the GO nanosheets embedded between the reference and working electrode within the polyamide membrane. The blue box, zooms in on a single nanosheet and depicts the constructed affinity assay for lactate. (For interpretation of the references to colour in this figure legend, the reader is referred to the Web version of this article.)

sweat [23]. Researchers have made efforts to develop non-invasive systems for measuring lactate in perspiration. Still, these systems necessitate the use of patches for sweat collection followed by laboratory analysis of the samples for lactate quantification. Such processing limits dynamic instantaneous feedback of the changes to the lactate concentration.

Most existing transdermal sweat biosensors need at least 10–100 μL of sweat in a localized region and rely on chemically or electrically stimulated sweating to achieve sufficient sample volume [24]. These efforts were followed by the use of pilocarpine stimulation of eccrine glands to produce elevated perspired sweat to enable dynamic monitoring from conformal epidermal form factor based sensors. While these sensors have shown promise in context to lactate monitoring in exercise physiology, it is unclear if the pilocarpine stimulation will support dynamic continuous monitoring from sedentary as well as mobility challenged population cohorts such as geriatric population and pediatric population under medical care. Therefore, to design a wearable sweat-based sensor that can measure and report interest biomarkers passively expressed from 1 to 5 μL volume is a big challenge [12,25,26].

Recent studies have reported several wearable electrochemical lactate biosensors for detection of lactate in tears [27] like real-time biosensors that could be applied as “tattoos” for monitoring of lactate in human sweat [12,24,28], and a mouth-guard-based biosensor for salivary lactate monitoring [29]. These lactate biosensors could continuously detect the lactate level in human body fluids in a non-invasive way. However, the results show a narrow dynamic range with a limit of detection of 20 mM [28]. Additionally, all the techniques require a large fluid volume of 10 μL for its operation.

As already mentioned, another challenge with the analysis of sweat is high lactate concentration which is typically 10 times higher than in blood. Lactate concentration in sweat of a healthy human is in the range from 4 to 25 mM [19,23,30,31], whereas after exercise it increases up to 80 mM [19,23,30], and under the ischemic conditions it can rise up to 62 ± 16.3 mM [20]. Therefore, the upper detection limit of lactate sensor in human sweat has to be at least 80–100 mM. However, the upper detection limits for most commercially available handheld lactate biosensors are of 20–25 mM [14,28], because it is designed for blood lactate detection, and it is not suitable for non-invasive monitoring. To overcome this drawback, several authors have reported upper detection limits of 70 mM and 180 mM in human sweat [26,32], but still need the use of redox molecules such as Prussian blue modified working electrodes to assist in detection.

In this work, for the first time we demonstrate lactate sensing from passively expressed eccrine sweat without the use of redox molecules. Instead, non-faradaic electrochemical impedance spectroscopy (EIS), highly suitable for low power wearable applications was used as a label-free method for fast and highly specific affinity-based detection of lactate without modifying the target molecule. Lactate oxidase (LOD) was used because of its simple reaction. LOD catalyzes the oxidation of lactate to pyruvate and forms hydrogen peroxide. Hydrogen peroxide is electrochemically active and can be oxidized to generate charged ions. Chemical and electrochemical reactions involved in a LOD sensor can be summarized by the following reactions:

$$\text{L– Lactate} + O_2 \xrightarrow{\text{L– lactate oxidase}} \text{pyruvate} + H_2O_2 \quad (1)$$

$$H_2O_2 \rightarrow O_2 + 2H^+ + 2e^- \quad (2)$$

Lactate detection mechanism was based on the production of charged ions in the enzymatic layer, as a result of L-lactate oxidation via LOD catalyzed reactions, which produces effective changes in the capacitive and resistive behaviors, and is monitored by electrochemical impedance spectroscopy (EIS).

Low-cost graphene oxide (GO) nanosheets were used in this work as a transduction element in a low-volume sensing platform with affinity-based detection mechanism. GO nanosheets were distributed within the pores of a porous polyamide (PA) membrane through use of vacuum over the sensing region of the electrode. The hydrophilic property of the PA membranes allows for less than 5 μL volume to cover the entire sensing region. The application of the dispersed GO nanosheets between vertically aligned electrodes allows for three-dimensional (3D) sensing. We have reported previously the use of 3D electrodes for detecting cortisol [25] which allows sensing across the membrane substrate as opposed to sensing in a 2D manner on the surface. A visual representation of the sensor is shown in Fig. 1a where the sensor's front end can non-invasively attach to the user's skin. Fig. 1b shows a schematic representation of the described assay construction for the sensor. The front electrode was designed in an open-face manner to introduce the fluid/biomolecules for constructing the lactate assay as well as lactate itself from sweat during sensing. In our study, due to the high surface-to-volume ratio of GO nanosheets, the upper detection limit of the sensor was increased even further to detect lactate in sweat across physiologically relevant concentrations. 1-Pyrenebutyric acid–N-hydroxysuccinimide ester (PANHS) was used as a linker molecule comprising of an anchor group and a terminal group. Its pyrene moiety interacts with the surface of the graphene by irreversible π – π stacking, while the protein substitutes the NHS moiety through nucleophilic attack, resulting in the formation of an amide bond [33]. This linker has been used successfully for the immobilization of glucose oxidase and

glutamic acid dehydrogenase [34,35]. To our knowledge, this work and our previous cortisol work with ZnO and MoS_2 are the only examples of non-faradaic, label-free sensing with the ability to detect the target molecule's temporal dynamics on a flexible substrate platform in human sweat [36].

Our present work on GO functionalized biosensing is the first proof of technological feasibility towards the development of a flexible biosensor for the real-time, continuous, and non-invasive monitoring of lactate in passively expressed human sweat. The performance of the sensor has been enhanced such that its active range matches the physiologically expressed range of lactate in human sweat. The premise of this paper is to demonstrate (1) The dynamic range of the lactate biosensor is found to be in between 1 mM and 100 mM, which has also been identified as the physiologically relevant range for sweat lactate reported by Sakharov et al. [23]. (2) Non-faradaic, label-free biosensor on a flexible substrate platform. We have also benchmarked the sensor's response with the commercially available Lactate Plus meter to prove the sensor performance.

2. Experimental section

2.1. Materials and reagents

Polyamide substrates with a pore size of 0.2 μm were purchased from GE Healthcare Life Sciences (Piscataway, NJ, USA). Solvent Dimethyl Sulfoxide (DMSO), and 150 mM Phosphate Buffered Saline (PBS) were ordered from Thermo Fisher Scientific Inc. (Waltham, MA, USA). The Sodium L-lactate and 1-pyrenebutyric acid–N-hydroxysuccinimide ester (PANHS) were ordered from Sigma (Co., USA). Lactate oxidase was ordered from Toyobo (USA INC.). Graphene oxide (GO) was purchased from Graphenea (San Sebastián, Spain). Synthetic sweat was prepared as per the recipe stated in M.T. Mathew et al. [37]. The pH range is varied by varying the concentration of the components and is adjusted by lactic acid and ammonia. Synthetic sweat solutions were prepared with pH = **4**, 6, and 8. Human sweat was purchased from Lee Biosolutions Inc. (St. Louis, MO, USA), where it was collected from single human donor with pH ~ 4–5. No preservatives have been added to this product and it was stored unfiltered at below −20 °C. All the lactate dilutions are made in synthetic sweat or human sweat.

2.2. Graphene oxide nanosheets preparation

GO nanosheets preparation was based on the breakage of GO by ultra-sonication processes. GO (4 mg/mL) was suspended in water and ultra-sonication treatment was applied at 6 h. The temperature of the water in the ultra-sonication bath was kept below 45 °C. The GO and sonicated GO nanosheets size were determined by Malvern ZetaSizer (Nano ZS, Malvern Instruments). The original size of GO is 5018 ± 362 nm. After 6 h of sonication, the average size is 726 ± 41 nm.

2.3. Sensor fabrication

The sensor stack consists of palladium electrodes. A two-step thin film cryo-evaporation deposition process using in-house fabricated shadow mask stencils was used to fabricate 100 nm palladium working and reference electrodes upon the polyamide membranes. The dimension of electrode sensing area is ~1 cm × 0.5 cm. AutoDesk™ AutoCAD was used to design electrode geometries. Stencils were fabricated using a Kapton sheets and were cut by a Spectra-Physics Spirit laser system. GO nanosheets was dispersed into porous PA membrane through vacuum assistance over the sensing region of the electrode, on the non-electrode deposited side of the membrane. 3 μL of 4 mg/mL GO solution was applied. After GO is dispersed into membrane, the second electrode pattern was deposited completing the fabrication processes. The back side shadow mask was aligned to the front side electrode using alignment marks and a backlit alignment platform.

2.4. Affinity assay functionalization and protocols

After sensor fabrication, 10 μL of 5 mM PANHS in dimethyl-sulfoxide (DMSO) was dispersed onto GO nanosheets and incubated for 1 h in dark. After a 10 μL PBS wash to remove any unbound PANHS crosslinker, 10 μL of 4 mg/mL lactate oxidase was applied and incubated for 3 h. Lactate-free synthetic sweat is dosed on the sensor prior to introducing the doses and is considered as the baseline. For the calibration dose response, 2–3 μL of lactate doses (1, 10, 50, 100 mM) prepared in synthetic sweat were dispensed on the sensing region and incubated for 3 min. EIS measurements record the current flow using a Potentiostat (Gamry Instruments, Warminster, PA, USA) after an AC excitation signal with frequency sweep of 1 Hz to 1 MHz is applied. Following doses were added from lowest concentration to highest, and were all incubated for the same 3 min before measurements were taken.

The continuous experiment is done by dispersing 15.4 mM of lactate in synthetic sweat to the sensing region progressively. Fifteen applications of the same dose concentration were added at a rate of 3 μL per 5 min (incubation time plus 2 min recording time) before moving to the next dose, this continued through 231 mM for a total duration of ~75 min.

For the cross-reactivity study, the cortisol was prepared in lactate-free synthetic sweat with the same concentration as lactate. 2–3 μL of cortisol doses (1, 10, 50, 100 mM) were dispensed on the sensing region and incubated for 3 min before measurement.

2.5. Infrared spectroscopy (ATR-FTIR)

Infrared spectra of GO, GO with PANHS, and functionalized GO nanosheets were recorded with a Thermo Scientific Nicole iS50 FT-IR using an Attenuated Total Reflectance (ATR) stage. The tool was equipped with a deuterated triglycine sulfate (DTGS) detector and KBr window. Attenuated Total Reflection (ATR) IR spectroscopy was performed using germanium crystal which has a mid-IR range covering 4000 and 600 cm^{-1} wavelengths. ATR-FTIR specimens were prepared by deposition the GO on PA membrane as substrate. The contact area was about 1 cm^2. All spectra were recorded between 4000 and 600 cm^{-1} with a resolution of 4 cm^{-1} and 64 scans.

3. Results and discussion

The organization of this section prearranged is as follows: (1) Structural characterization and functionalization of the developed sensor for lactate sensing; (2) Optimization of frequency for sensor operation; (3) pH study on graphene oxide electrode; (4) LOD activity on the GO sensor electrode in different pH buffer; (5) Sensor calibration dose response of lactate in synthetic sweat; (6) Continuous detection of lactate; (7) Lactate detection in low-volume perspired human sweat; (8) Comparison of sensor performance in synthetic sweat with Lactate Plus meter.

4. Structural characterization and functionalization of the developed sensor for lactate sensing

Fig. 2a shows the Scanning Electron Microscopy (SEM) image of GO nanosheets dispersed onto the porous polyamide (PA) substrate to study the distribution of the GO nanosheets. The GO nanosheets were observed not only on top of the PA membrane, but also inside the porous membrane. Based on the result of Zeta sizer (supplementary), the average size of GO nanosheets after 6 h sonication is 726 ± 41 nm. Although this size is larger than nominal pore size of PA membrane, which is 200 nm, we observed many smaller GO nanosheets were inside the nanopores as shown in the inset of Fig. 2a. Greater surface area can be used for enzyme immobilization by dispersing more GO nanosheets into nanopores, and thus increase the dynamic range of detection. Fig. 2b and Table 1 show chemical characterization using ATR-Fourier

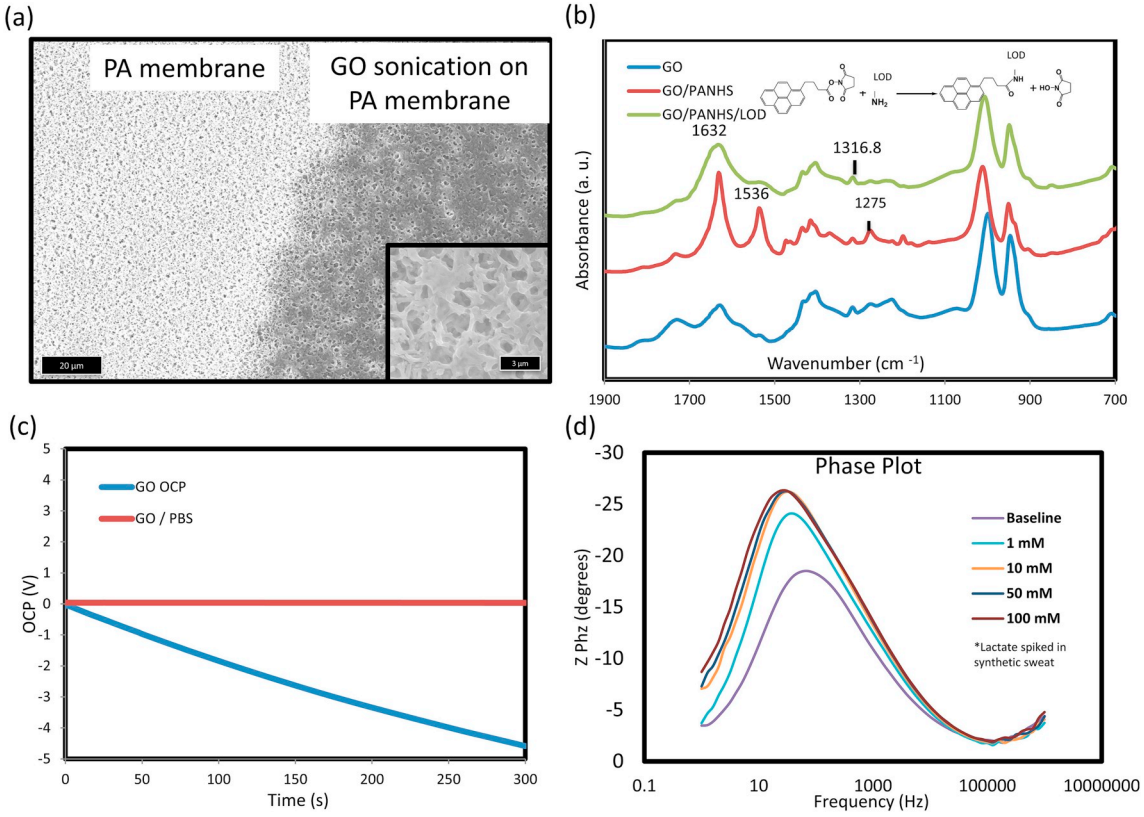

Fig. 2. (a) SEM image of blank polyamide membrane (left) and GO nanosheets deposited into porous polyamide membrane (right). (**b)** ATR-FTIR spectra for the construction of the lactate assay showing: (Blue) GO, (Red) GO + PANHS, and (Green) GO + PANHS + LOD. (c) Open circuit potential curves of GO electrode without and with PBS buffer. GO electrode shows stable potential in PBS buffer over time. (d) Phase plot for lactate dose response. (For interpretation of the references to colour in this figure legend, the reader is referred to the Web version of this article.)

Table 1
ATR-FTIR peak identification and assignment for assay functionalization steps.

Mode assignment	Peak Position (cm^{-1})		
	GO	GO + PANHS	GO + PANHS + LOD
C–O	998	1012	1006
O–H	1404	1404	1404
C–C	1632	1632	1632
C–N–C	N/A	1275	Shift to1316.8
Second amide	N/A	1536	Disappear

Transform Infrared Spectroscopy (ATR-FTIR) to confirm the binding of PANHS and subsequently of lactate oxidase (LOD) during sensor functionalization on the GO nanosheets. Post-PANHS incubation, the appearance of IR bands corresponding to C–N–C stretching modes (at 1275 cm^{-1}) and secondary amide (at 1536 cm^{-1}) indicate the formation of the PANHS monolayer. Secondly, after the LOD incubation, the 1536 cm^{-1} and 1275 cm^{-1} peaks disappear, indicating the detachment of the succinimidyl group (NHS) from the PANHS layer. The C–N–C stretching mode shifts to 1316.8 cm^{-1} suggesting that LOD was successfully conjugated to the PANHS. This confirms that PANHS and LOD are bound to the GO nanosheet surface. Fig. 2c shows the open circuit potential (OCP) value of GO electrode with and without PBS buffer. The potential stability of GO nanosheet embedded electrode is demonstrated in PBS over 300 s indicating potential is stable during the measurement.

4.1. Optimization of frequency for sensor operation

Non-faradaic EIS measurements quantify the binding interactions of LOD and lactate based on mainly the impedance changes that occur at the electrical double layer (EDL) due to change in the dielectric permittivity. The Bode phase plot (Fig. 2d) of the lactate oxidase (LOD) and lactate showed a phase lag of 10–30° which indicated the resistive behavior of the sensor. Z_{mod} reflects the total impedance of both capacitive and resistance of the system. The total impedance (Z_{mod}) variations were analyzed over frequencies from 1 Hz to 1 MHz with a small AC excitation signal. The highest signal-to-noise ratio (SNR) was obtained between 5 and 50 Hz frequency. In this range the resistive nature was dominant, which indicates that the GO transduction element is most sensitive to electrochemical process through charge transfer mechanisms (R_{ct}). (The equivalent Randle's circuit and R_{ct} will be discussed in *Sensor calibration dose response of lactate in synthetic sweat* session). The formation of an affinity immunoassay on a carbon-based material i.e. GO surface in this case, resulted in an increase in impedance with increased dose of lactate. The noise variation was most stable at 10 Hz; therefore, it was used for the sensor stability study and calibration in synthetic sweat.

4.2. pH study on graphene oxide electrode

We first evaluated the stability of GO nanosheet electrode over the range of pH conditions found in human sweat, then performed studies to evaluate the stability of LOD enzyme at varying pHs. Since the pH of human sweat varies from pH = **4.5 to** pH = **8.0**, we formulated synthetic sweat (SS) with different pH at 4, 6, and 8 to span this range. Fig. 3a shows the variations in Z_{mod} of each pH solution. The Z_{mod} in pH = **8** solutions SS was 3106 Ω whereas in pH = **6 and** pH = **4** was 2616 Ω and 2222 Ω. A total of n = 3 replicates were performed and a p value greater than 0.05 was obtained for all pH conditions with respect to the impedance value obtained in the synthetic sweat. The lower

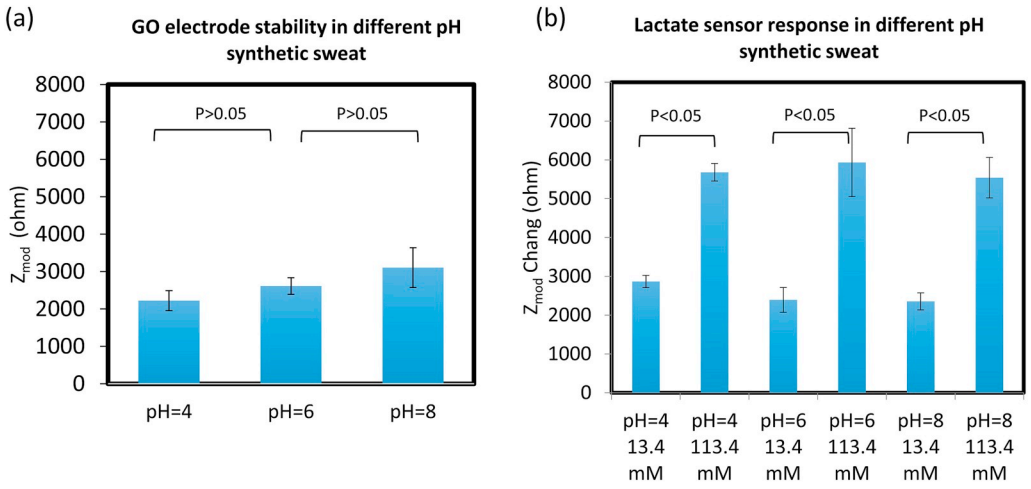

Fig. 3. pH study on graphene oxide electrode (**a**) The variations in Z_{mod} of each pH solution. The impedance values for each pH solution are statistically insignificant compared to the impedance obtained from different pH solution. (**b**) The variations in Z_{mod} change of each pH solution with respect to the baseline Z_{mod} of each pH solution. The baseline was measured in the synthetic sweat without lactate. p-values depicted are the comparison of the statistical significance between the measurements in low and high lactate concentration.

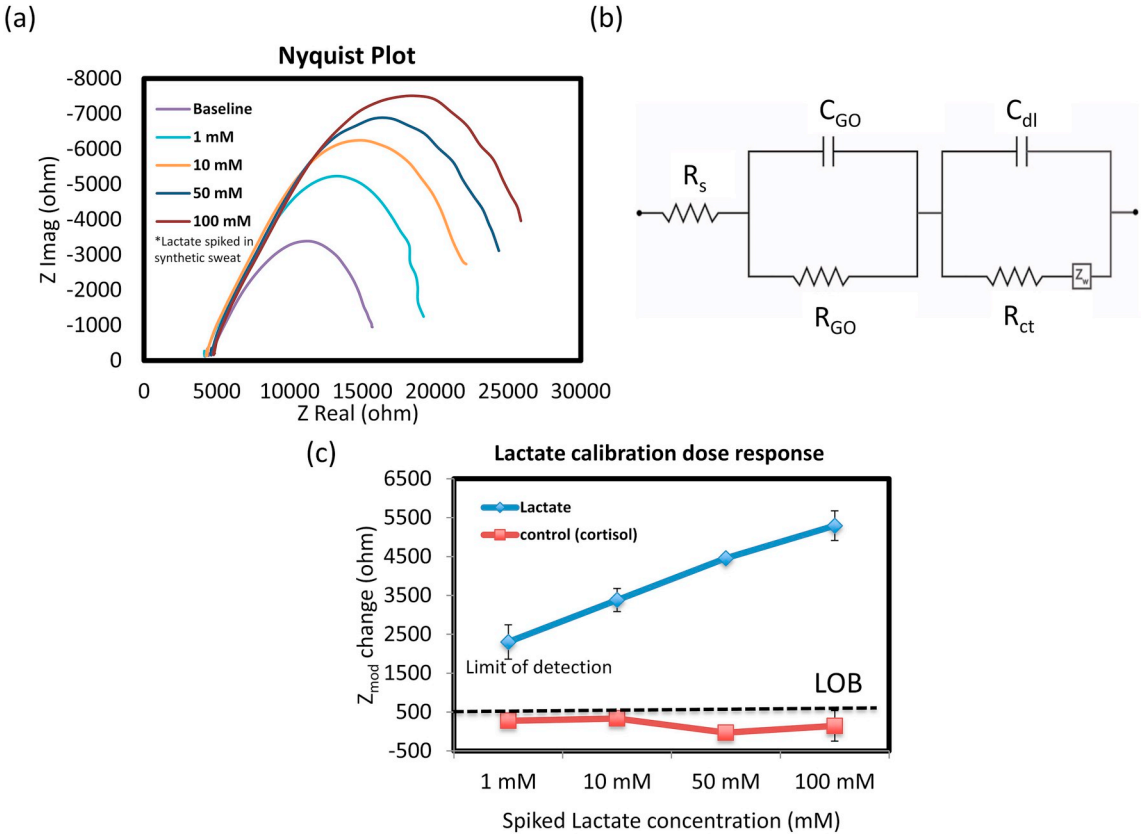

Fig. 4. (a) Nyquist plot for lactate dose response. (**b**) Modified Randles circuit representing the GO functionalized electrode system comprised of passive electrical components. (**c**) (blue) Lactate calibration dose response showing change in impedance with respect to the post-antibody baseline measurement for 1, 10, 50, and 100 mM of lactate in synthetic sweat (n = 3). (red) Cortisol crowss-reactivity study (n = 3). (Dotted black) Limit of Blank. Error bars are Standard Error of Mean. (For interpretation of the references to colour in this figure legend, the reader is referred to the Web version of this article.)

value in Z_{mod} at low pH solution can be attributed to the H^+ charge screening effect along the GO electrode surface, and the H^+ charge interfered with the electron-charge transfer. Overall the variations in Z_{mod} of each pH solution from pH = **4 to** pH = **8** are less than 1 kΩ. This change was within the system signal threshold, also known as the noise threshold.

5. LOD activity on the GO sensor electrode in different pH buffer

The enzyme activity of the lactate oxidase functionalized GO sensor was also examined in different pHs of synthetic sweat after enzyme immobilization. Lactate concentration of 100 mM was spiked in synthetic sweat solution of pH = **4**, 6 and 8. The synthetic sweat had a baseline 13.4 mM of lactic acid in solution. The final lactate concentrations tested in varying pH synthetic sweat solutions were 13.4 mM and 113.4 mM. Fig. 3b shows the variations in Z_{mod} change for each pH solution with respect to the baseline Zmod of each pH solution. The baseline was measured in the synthetic sweat without lactate. A total of $n = 3$ replicates was performed and a p-value smaller than 0.05 was obtained between low (13.4 mM) and high (113.4 mM) lactate concentration for all pH conditions with respect to the impedance value obtained in the synthetic sweat. The change in Z_{mod} for 13.4 mM lactate

concentration in pH = **8** solutions of SS was 2356 Ω (35.8% changed compared to baseline), whereas in pH = **6 and** pH = **4** solutions were 2393 Ω (36.4% changed compared to baseline) and 2866 Ω (41.9% changed compared to baseline) respectively. At 113.4 mM lactate concentration, the change in Z_{mod} for SS of pH = **8** was 5539 Ω (84.7% changed compared to baseline), whereas in pH = **6 and** pH = **4** solutions the impedance changes were 5933 Ω (89.1% changed compared to baseline) and 5679 Ω (84.2% changed compared to baseline) respectively. These changes also demonstrate that the dynamic range of lactate in human sweat can be detected across the varying pH ranges of 4 through 8.

5.1. Sensor calibration dose response of lactate in synthetic sweat

We tested different dose concentrations of lactate in the physiologically relevant range in human sweat of 1, 10, 50, and 100 mM spiked in synthetic sweat on independent lactate oxidase immobilized sensors to establish the impedance-concentration correlation for creating calibration dose response curve. As earlier mentioned in Fig. 2d, the Bode phase plot of the lactate oxidase (LOD) and lactate showed a phase lag of 10–30° which indicated the resistive behavior of the sensor. Z_{mod} reflects the total impedance of both capacitive and resistance of the system, so Z_{mod} is a prudent measure to evaluate sensor performance. Fig. 4a shows the Nyquist plot of lactate detection from 1 mM to 100 mM lactate spiked in synthetic sweat. The region occurring at 1 MHz begins at an offset of approximately 4.5 KΩ on the Z_{real} axis as indicated in Fig. 4a. The offset corresponds to solution resistance (R_s) as represented in the equivalent circuit shown in Fig. 4b. This region shows an increase in the semicircle radius with increasing dose concentration. There is an increase both in Z_{real} and Z_{imag} part with respect to increasing lactate concentration. The change in Z_{mod} corresponding to increased binding events is confirmed by the change in Z_{real} observed in the Fig. 4a, proving that both accurately serve as measures which can be used to verify sensor performance.

The increase in R_{ct} and R_{GO} is due to the lactate binding on the GO nanosheets blocking charge transfer. Table 2 summarized the theoretical fits of the experimental results of all the capacitive and resistive components. Z-view software was used to fit the modified Randle's circuit. The fitted result shows 71.3% increase in R_{ct} as lactate concentration increased from 0 to 100 mM. R_{GO} also increases with 228% as dosage concentration increase from 0 to 100 mM. In addition, the EDL capacitance (C_{GO}) also increases, but is stable after 10 mM lactate. Overall, R_{ct} and R_{GO} are the two major components of the equivalent circuit which dominate the dose response and imply that the sensor is sensing resistive changes generated by lactate binding to the GO nanosheets.

The calibration dose response (CDR) of the sensor is shown in Fig. 4c as a change in Z_{mod} impedance from the baseline measurement post-LOD functionalization at 10 Hz for n = 3 replicates. There is a monotonic increase in impedance as the dosage concentration of lactate increases. The calibration dose response for lactate concentrations of 1 mM, 10 mM, 50 mM, and 100 mM lactate spiked in synthetic sweat is shown in Fig. 4c. An impedance change from 2303 ± 442 Ω to 5293 ± 379 Ω was observed for the concentration from 1 mM to 100 mM. Cortisol was used as a cross-reactive molecule to examine the specificity of the system. Cortisol is released in blood, saliva and sweat in response to stress and low blood-glucose concentration. Cortisol is also a common biomarker in sweat and can be used as a cross-reactive molecule for this study. The same protocol was used as for lactate, but with doses of cortisol, while retaining the lactate oxidase. The response shown in Fig. 4c shows impedance changes that are within the noise threshold for all concentrations of cortisol. Therefore, the sensor is not affected by the non-specific adsorption associated with cortisol. This validates that the change in impedance is a function of lactate specifically binding to functionalized GO. Thus, with the Limit of Blank ($LOB = mean_{blank} + 1.645*(SD_{blank})$) (SD: standard deviation) calculated as 449.1 Ω, the limit of detection of 1 mM lactate spiked in synthetic sweat can be established.

Table 2
Theoretical fit of experimental results for the capacitive and resistive electrical components of the Modified Randles Circuit.

Spiked Lactate concentration (mM)	R_{sol} (ohm)	R_{GO} (ohm)	C_{GO} (nF)	R_{ct} (ohm)	C_{dl} (nF)
0	4475	1897	0.8	9125	1.58
1	4129	3242	2.54	12,358	1.67
10	4180	3319	3.38	15,458	1.88
50	4511	5258	3.29	14,894	2.00
100	4684	6219	3.29	15,633	2.19

5.2. Continuous detection of lactate

Fig. 5a represents the continuous response of the sensor for a lactate concentration of 15.4 mM in synthetic sweat for each dosing step. Lactate spiked in synthetic sweat were applied at a rate of 3 μL (4.2 ng lactate) every 5 min to the sensor. This protocol was used from a modified protocol previously reported by our group [25,38]. An incremental change in impedance was observed with increasing dose concentrations of lactate until 37.5 ng (138.6 mM). After 37.5 ng lactate, the change in impedance started to decrease showing that sensor was saturated and excess lactate molecules acting as free ions caused the decreasing impedance change. This suggests that the sensor is responsive to concentrations of lactate up to ~138.6 mM over at least 45 min and is suitable for continuous sensing at high levels of lactate from low volumes of synthetic sweat.

5.3. Lactate detection in low-volume perspired human sweat

The calibration data of sensor performance in human sweat spiked with lactate dose concentration is shown in Fig. 5b for $n = 5$ replicates (except 100 mM dose for n = 3). The Z_{mod} change in impedance varied from 785.8 ± 94 Ω (10.8% increase compared to human sweat baseline) to 1876 ± 329 Ω (25.7% increase compared to human sweat baseline) for logarithmic dilutions of lactate doses ranging from 1 to 100 mM. In comparison to the calibration data obtained for synthetic sweat solutions (Fig. 4c), the higher noise and lower Z_{mod} change are observed. We hypothesize this trend of lower impedance change is due to the ionic interferents present in human sweat. Additionally, the baseline lactate concentration present in human sweat was unknown. The only information form the literature is that lactate concentration in sweat of a healthy human is in the range from 4 to 25 mM [19,23,30,31], whereas after exercise it increases up to 80 mM [19,23,30]. As the human sweat obtained for testing on the sensor was collected through mild/moderate exercise by the vendor; hence the real concentration of lactate in human sweat when spiked with 100 mM of lactate may vary from 104 mM to 180 mM. Hence, the relatively high standard deviation at 100 mM dose may be attributed to the steric hindrance effects due to extremely high doses of lactate on the sensors.

5.4. Comparison of sensor performance in synthetic sweat with Lactate Plus meter

In order to compare and benchmark the performance of the sweat sensor, we chose Lactate Plus meter and strips from Nova Biomedical (Waltham, MA USA), a commercially available diagnostic tool for measuring lactate. 20 strips were tested for this analysis at concentrations of 1.3 mM, 4.7 mM, 10 mM, 18.4 mM, and 63.4 mM concentrations of lactate. 4 of 20 showed error data, and 3 of 20 were shown out of range (63.4 mM). To quantify the correlation between two methods of measurements, two types of analysis were used and tested in synthetic sweat: (1) R^2 –value of regression analysis for the correlation

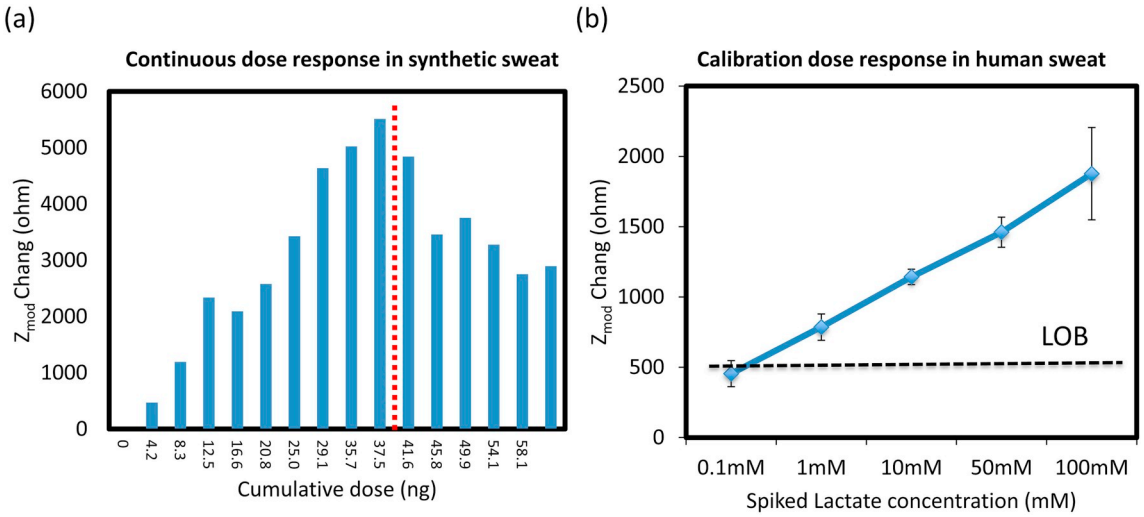

Fig. 5. (a) Continuous detection of lactate in synthetic sweat. Lactate drops were applied at a rate of 3 μL (4.2 ng lactate) every 5 min to the sensor. Change in impedance responded incrementally to the increasing dose of lactate until 37.5 ng. **(b)** Lactate calibration dose response in human sweat. (blue) Change in impedance with respect to the post-antibody human sweat baseline measurement for 0.1, 1, 10, 50, and 100 mM of lactate in synthetic sweat (n = 5 for 0.1–50 mM, n = 3 for 100 mM). (Dotted black) Limit of Blank. Error bars are Standard Error of Mean. (For interpretation of the references to colour in this figure legend, the reader is referred to the Web version of this article.)

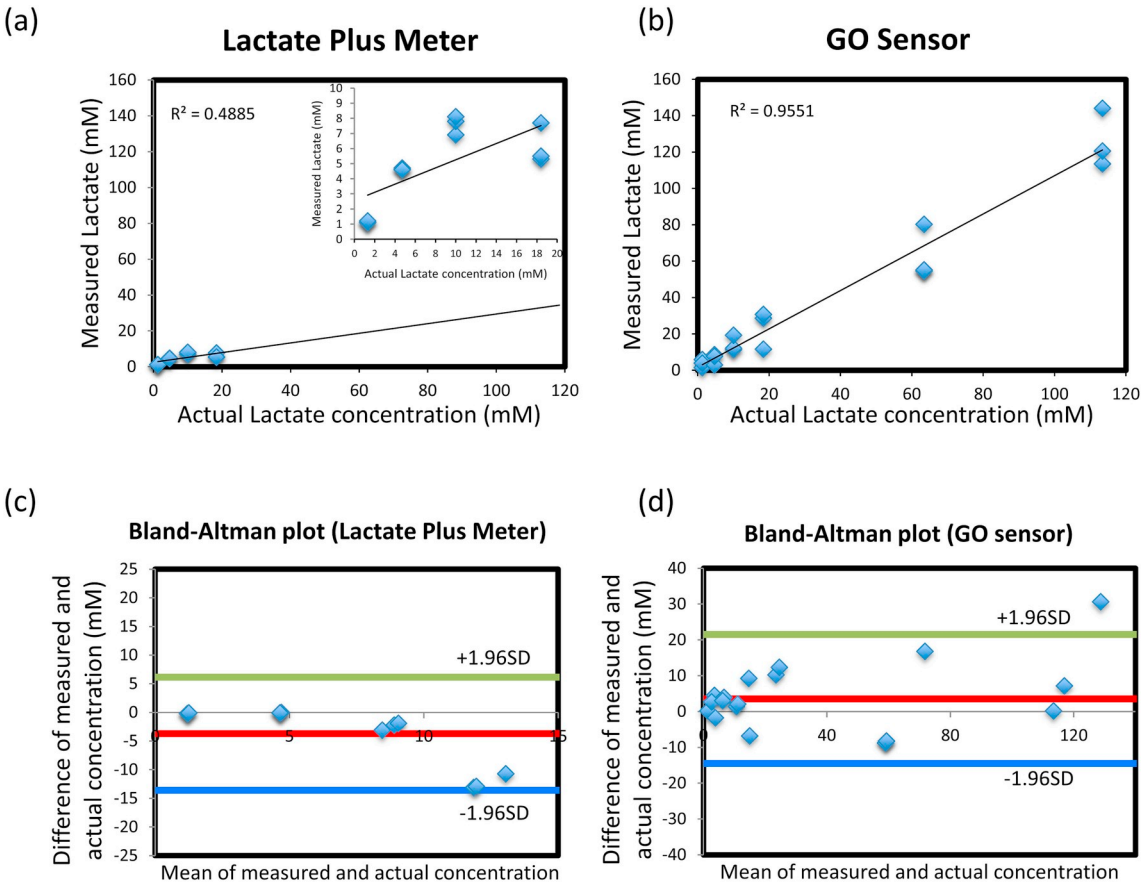

Fig. 6. (a) (b) Comparison of Lactate Plus meter and developed GO sensor using regression analysis for test samples. The inset of 6 (a) shows lactate concentration from 1 to 20 mM. The tested lactate concentration higher than 20 mM of Lactate Plus meter were shown out of range (63.4 mM). (c) (d) Comparison of Lactate Plus meter and developed GO sensor using Bland-Altman plot for test samples.

between the response of the GO sweat sensor under development and the response from the Lactate Plus meter. (2) Bland-Altman analysis for the response of the GO sweat sensor under development and the response from the Lactate Plus meter. Fig. 6a is the correlation plot representation of the measurements from Lactate Plus meter to the known lactate concentrations. The meter showed an R^2 value of 0.9583 at 1.3–10 mM lactate range. By including the Lactate Plus meter response at 18.4 mM, the regression analysis resulted in a R^2 value of 0.4885, indicating that the Lactate Plus meter drifts at lactate concentrations above 10 mM. Fig. 6b shows the correlation plot representation of the

measurements from GO sensor to the known lactate concentrations. GO sensor showed an R^2 value of 0.9551 within the 1.3–113.4 mM lactate range. These results indicate that the GO sweat sensor has a wide linear dynamic range of operation that spans across the entire physiological range of sweat lactate. Thus, sweat-based lactate sensing is a promising technology for monitoring the temporal changes to lactate when the sensor is implemented in a wearable form factor.

Bland-Altman analysis was performed to analyze the agreement between the responses obtained from two different types of measurements or devices namely the GO sweat sensor and the Lactate Plus meter. As the dynamic region of response from Lactate Plus meter was much smaller than the GO sensor, Bland-Altman analysis was performed to compare responses from both the Lactate Plus meter and GO sensor to known spiked lactate levels in synthetic sweat over the concentration range over to which the individual devices demonstrate a linear response. Fig. 6c shows the Lactate Plus meter response in comparison to a known lactate concentration at 1.3–20 mM concentration range where the mean bias is 3.71 mM and SD of bias (1.96*SD) is 5.04 mM. Fig. 6d shows the GO sensor's response in comparison to a known lactate concentration over the concentration range of 1.3–113.4 mM where the mean bias is 3.53 mM and SD of bias (1.96*SD) is 9.18 mM. On analyzing the GO sensor's response within the 1.3–20 mM lactate range so as to draw a comparison with the Lactate Plus meter, we found the mean bias and the SD of the bias to have changed to 3.43 mM and 5.09 mM respectively, which is only 0.28 mM difference of mean bias from the result obtained on the Lactate Plus meter. The biases between the measurements done on GO sensor and known lactate concentration are distributed on both sides of mean bias as observed in Fig. 6d. The value of bias is 3.53 mM which lies close to zero. Similar results were produced by the GO sensor. Almost all the measurements were within ±1.96SD of the mean bias except one data point collected from the GO sensor at 113.4 mM lactate concentration. Overall, the analysis indicates the GO sensor and Lactate Plus meter have similarity in their results within 1.3–20 mM lactate concentration range, and GO sensor demonstrates a wider dynamic range within the 1.3–113.4 mM concentration. The Bland-Altman analysis indicates that the GO sensor performs within 5% deviation of the Lactate Plus sensor over the dynamic concentration range of the Lactate Plus sensor i.e. from 1.3 mM to 113.4 mM of lactate. Additionally, the GO Sensor does not drift in its performance over the larger dynamic range i.e. ranging from 20 mM to 113.4 mM, with the exception of the 113.4 mM where the standard deviation is increased presumably due to steric hindrance.

6. Conclusion

Lactate monitoring has tremendous importance in the field of exercise training and diabetes control [39]. In this study, detection of lactate in appropriate ranges of perspired human sweat was established at low volume (<5 μL) using a crossing membrane metal electrode sensor system in combination with graphene oxide nanosheets. The sensing ability was done by measuring impedance changes associated with lactate binding to the lactate oxidase at the GO nanosheet interface using electrochemical impedance spectroscopy. Lactate oxidase was immobilized on the GO nanosheets as the active sensing element. The sensor demonstrated a dynamic range of spiked lactate in synthetic sweat from 1 to 100 mM with a limit of detection of 1 mM. Continuous dosing studies demonstrated the sensor's ability to response concentrations of lactate up to 138.6 mM over 45 min, and consequently is suitable for continuous sensing at high levels of lactate from low volumes of sweat. Sensor specificity was established through a cross-reactivity study using cortisol. This study also analyzed the sensor performance using Bland-Altman analysis and regression analysis to evaluate the efficacy of sensor calibration and accuracy of detection of lactate in synthetic sweat. Overall, there is limited variability in lactate detection from synthetic sweat and wider dynamic range compared to commercial Lactate Plus meter. For the further study, there are still many challenges ahead needed to be solved, such as changes in dielectric strength, pH and conductivity of body fluids. We expect this work will inspire research and development in this area.

Authorship contributions

Kai-Chun Lin (KL) contributed to this work in establishing protocols, producing the data represented in this manuscript, and in the writing of the manuscript itself. KL also performed the sensor characterization studies. Sriram Muthukumar (SM) and Shalini Prasad (SP) conceptualized this work, the design of the sensors and experiments, critical revision of protocols, analysis of data, and supervision of the project.

Competing financial interests

Drs. Shalini Prasad and Sriram Muthukumar have a significant interest in Enlisense LLC, a company that may have a commercial interest in the results of this research and technology. The potential individual conflict of interest has been reviewed and managed by The University of Texas at Dallas, and played no role in the study design; in the collection, analysis, and interpretation of data; in the writing of the report, or in the decision to submit the report for publication. Dr. Lin declares no potential conflict of interest.

Non-financial competing interests

The authors declare no non-financial competing interests.

Acknowledgements

We thank the Cecil and Ida Green endowment in Systems Biology at the University of Texas at Dallas and Enlisense LLC for their financial support in this work. The authors would like to thank Badrinath Jagannath for his help with Z-view fitting of the Nyquist data and also thank David Kinnamon for his help with fabrication the sensors based on concept design.

Appendix A. Supplementary data

Supplementary data to this article can be found online at https://doi.org/10.1016/j.talanta.2020.120810.

References

[1] L.B. Gladden, Lactate metabolism: a new paradigm for the third millennium, J Physiol-London 558 (1) (2004) 5–30.
[2] C.C. Webster, T.D. Noakes, S.K. Chacko, J. Swart, T.A. Kohn, J.A.H. Smith, Gluconeogenesis during endurance exercise in cyclists habituated to a long-term low carbohydrate high-fat diet, J Physiol-London 594 (15) (2016) 4389–4405.
[3] J. Bakker, P. Gris, M. Coffernils, R.J. Kahn, J.L. Vincent, Serial blood lactate levels can predict the development of multiple organ failure following septic shock, Am. J. Surg. 171 (2) (1996) 221–226.
[4] B.A. Mizock, J.L. Falk, Lactic-acidosis in critical illness, Crit. Care Med. 20 (1) (1992) 80–93.
[5] G.A. Brooks, W.C. Stanley, E.W. Gertz, J.A. Wisneski, D.L. Morris, R.A. Neese, Systemic lactate kinetics during graded-exercise in man, Med. Sci. Sports Exerc. 17 (2) (1985) 206-206.
[6] K. Svedahl, B.R. MacIntosh, Anaerobic threshold: the concept and methods of measurement, Can. J. Appl. Physiol. 28 (2) (2003) 299–323.
[7] M.R. Romero, F. Ahumada, F. Garay, A.M. Baruzzi, Amperometric biosensor for direct blood lactate detection, Anal. Chem. 82 (13) (2010) 5568–5572.
[8] W.S. Simonides, R. Zaremba, C. Vanhardeveld, W.J. Vanderlaarse, A nonenzymatic method for the determination of picomole amounts of lactate using hplc - its application to single muscle-fibers, Anal. Biochem. 169 (2) (1988) 268–273.
[9] S. Biagi, S. Ghimenti, M. Onor, E. Bramanti, Simultaneous determination of lactate and pyruvate in human sweat using reversed-phase high-performance liquid chromatography: a noninvasive approach, Biomed. Chromatogr. 26 (11) (2012) 1408–1415.
[10] L. Rassaei, W. Olthuis, S. Tsujimura, E.J. Sudholter, A. van den Berg, Lactate

biosensors: current status and outlook, Anal. Bioanal. Chem. 406 (1) (2014) 123–137.
[11] A.J. Bandodkar, J. Wang, Non-invasive wearable electrochemical sensors: a review, Trends Biotechnol. 32 (7) (2014) 363–371.
[12] T. Guinovart, A.J. Bandodkar, J.R. Windmiller, F.J. Andrade, J. Wang, A potentiometric tattoo sensor for monitoring ammonium in sweat, Analyst 138 (22) (2013) 7031–7038.
[13] J. Kim, W.R. de Araujo, I.A. Samek, A.J. Bandodkar, W.Z. Jia, B. Brunetti, T.R.L.C. Paixao, J. Wang, Wearable temporary tattoo sensor for real-time trace metal monitoring in human sweat, Electrochem. Commun. 51 (2015) 41–45.
[14] W. Gao, S. Emaminejad, H.Y.Y. Nyein, S. Challa, K.V. Chen, A. Peck, H.M. Fahad, H. Ota, H. Shiraki, D. Kiriya, D.H. Lien, G.A. Brooks, R.W. Davis, A. Javey, Fully integrated wearable sensor arrays for multiplexed in situ perspiration analysis, Nature 529 (7587) (2016) 509–+.
[15] N.A. Taylor, C.A. Machado-Moreira, Regional variations in transepidermal water loss, eccrine sweat gland density, sweat secretion rates and electrolyte composition in resting and exercising humans, Extreme Physiol. Med. 2 (1) (2013) 4.
[16] P.M. Snezha Zlateva, Yulichka sabeva, Determination of toxic substances in sweat secret of severe forms of poisoning - toxic coma. clinical meaning, J.IMAB - Annual Proceeding (Scientific Papers) 13 (1) (2007) 86–88.
[17] N. De Giovanni, N. Fucci, The current status of sweat testing for drugs of abuse: a review, Curr. Med. Chem. 20 (4) (2013) 545–561.
[18] P.A. Pilardeau, M.T. Chalumeau, P. Harichaux, P. Vasseur, J. Vaysse, M. Garnier, Effect of physical-training on exercise induced sweating in men, J. Sports Med. Phys. Fit. 28 (2) (1988) 176–180.
[19] K. Mitsubayashi, M. Suzuki, E. Tamiya, I. Karube, Analysis of metabolites in sweat as a measure of physical condition, Anal. Chim. Acta 289 (1) (1994) 27–34.
[20] A. Polliack, R. Taylor, D. Bader, Sweat analysis following pressure ischaemia in a group of debilitated subjects, J. Rehabil. Res. Dev. 34 (3) (1997) 303–308.
[21] P.J. Derbyshire, H. Barr, F. Davis, S.P.J. Higson, Lactate in human sweat: a critical review of research to the present day, J. Physiol. Sci. 62 (6) (2012) 429–440.
[22] M.M. Pribil, G.U. Laptev, E.E. Karyakina, A.A. Karyakin, Noninvasive hypoxia monitor based on gene-free engineering of lactate oxidase for analysis of undiluted sweat, Anal. Chem. 86 (11) (2014) 5215–5219.
[23] D.A. Sakharov, M.U. Shkurnikov, M.Y. Vagin, E.I. Yashina, A.A. Karyakin, A.G. Tonevitsky, Relationship between lactate concentrations in active muscle sweat and whole blood, Bull. Exp. Biol. Med. 150 (1) (2010) 83–85.
[24] J. Kim, W.R. de Araujo, I.A. Samek, A.J. Bandodkar, W. Jia, B. Brunetti, T.R.L.C. Paixão, J. Wang, Wearable temporary tattoo sensor for real-time trace metal monitoring in human sweat, Electrochem. Commun. 51 (2015) 41–45.
[25] D. Kinnamon, R. Ghanta, K.C. Lin, S. Muthukumar, S. Prasad, Portable biosensor for monitoring cortisol in low-volume perspired human sweat, Sci Rep-Uk 7 (2017).
[26] M. Onor, S. Gufoni, T. Lomonaco, S. Ghimenti, P. Salvo, F. Sorrentino, E. Bramanti, Potentiometric sensor for non invasive lactate determination in human sweat, Anal. Chim. Acta 989 (2017) 80–87.
[27] H.F. Yao, A.J. Shum, M. Cowan, I. Lahdesmaki, B.A. Parviz, A contact lens with embedded sensor for monitoring tear glucose level, Biosens. Bioelectron. 26 (7) (2011) 3290–3296.
[28] W.Z. Jia, A.J. Bandodkar, G. Valdes-Ramirez, J.R. Windmiller, Z.J. Yang, J. Ramirez, G. Chan, J. Wang, Electrochemical tattoo biosensors for real-time noninvasive lactate monitoring in human perspiration, Anal. Chem. 85 (14) (2013) 6553–6560.
[29] J. Kim, G. Valdes-Ramirez, A.J. Bandodkar, W.Z. Jia, A.G. Martinez, J. Ramirez, P. Mercier, J. Wang, Non-invasive mouthguard biosensor for continuous salivary monitoring of metabolites, Analyst 139 (7) (2014) 1632–1636.
[30] X. Cai, J.L. Yan, H.H. Chu, M.S. Wu, Y.F. Tu, An exercise degree monitoring biosensor based on electrochemiluminescent detection of lactate in sweat, Sensor. Actuator. B Chem. 143 (2) (2010) 655–659.
[31] J.M. Green, R.C. Pritchett, T.R. Crews, J.R. McLester, D.C. Tucker, Sweat lactate response between males with high and low aerobic fitness, Eur. J. Appl. Physiol. 91 (1) (2004) 1–6.
[32] E.L. Tur-Garcia, F. Davis, S.D. Collyer, J.L. Holmes, H. Barr, S.P.J. Higson, Novel flexible enzyme laminate-based sensor for analysis of lactate in sweat, Sensor. Actuator. B Chem. 242 (2017) 502–510.
[33] R.J. Chen, Y.G. Zhang, D.W. Wang, H.J. Dai, Noncovalent sidewall functionalization of single-walled carbon nanotubes for protein immobilization, J. Am. Chem. Soc. 123 (16) (2001) 3838–3839.
[34] Y.X. Huang, X.C. Dong, Y.M. Shi, C.M. Li, L.J. Li, P. Chen, Nanoelectronic biosensors based on CVD grown graphene, Nanoscale 2 (8) (2010) 1485–1488.
[35] J. Tian, P.X. Yuan, D. Shan, S.N. Ding, G.Y. Zhang, X.J. Zhang, Biosensing platform based on graphene oxide via self-assembly induced by synergic interactions, Anal. Biochem. 460 (2014) 16–21.
[36] R.D. Munje, S. Muthukumar, A. Panneer Selvam, S. Prasad, Flexible nanoporous tunable electrical double layer biosensors for sweat diagnostics, Sci. Rep. 5 (2015) 14586.
[37] M.T. Mathew, E. Ariza, L.A. Rocha, A.C. Fernandes, F. Vaz, TiCxOy thin films for decorative applications: tribocorrosion mechanisms and synergism, Tribol. Int. 41 (7) (2008) 603–615.
[38] R.D. Munje, S. Muthukumar, S. Prasad, Lancet-free and label-free diagnostics of glucose in sweat using Zinc Oxide based flexible bioelectronics, Sensor. Actuator. B Chem. 238 (2017) 482–490.
[39] J.P. Talasniemi, S. Pennanen, H. Savolainen, L. Niskanen, J. Llesivuori, Analytical investigation: assay of D-lactate in diabetic plasma and urine, Clin. Biochem. 41 (13) (2008) 1099–1103.